OXFORD

Investigation of enhanced hemocompatibility and tissue compatibility associated with multi-functional coating based on hyaluronic acid and Type IV collagen

Jingan Li[1], Kun Zhang[1,2,3], Wenyong Ma[1], Feng Wu[1], Ping Yang[1,*], Zikun He[1] and Nan Huang[1]

[1]Key Laboratory for Advanced Technologies of Materials, Ministry of Education, School of Material Science and Engineering, Southwest Jiaotong University, Chengdu 610031, People's Republic of China; [2]School of Life Science, Zhengzhou University, 100 Science Road, Zhengzhou 450001, People's Republic of China and [3]Center of Stem Cell and Regenerative Medicine, First Affiliated Hospital of Zhengzhou University, 40 University Road, Zhengzhou 450052, People's Republic of China

*Correspondence address: Key Laboratory for Advanced Technologies of Materials, Ministry of Education, School of Material Science and Engineering, Southwest Jiaotong University, Chengdu 610031, PR China. Tel: +86-28-8763-4148-802; Fax: +86-28-87600625; E-mail: yangping8@263.net

Abstract

The biocompatibility of cardiovascular devices has always been considered crucial for their clinical efficacy. Therefore, a biofunctional coating composed of Type IV collagen (ColV) and hyaluronan (HA) was previously fabricated onto the titanium (Ti) substrate for the application of promoting vascular smooth muscle cell contractile phenotype and improving surface endothelialization. However, the anti-inflammation property, blood compatibility and *in vivo* tissue compatibility of the HA/ColV coating, as paramount consideration of cardiovascular materials surface coating, have not been investigated. Thus, in this study, the three crucial properties of the HA/ColV coating were tested. The platelet adhesion/activation test and the dynamic whole blood experiment implied that the HA/ColV coating had better blood compatibility compared with Ti substrate and pure ColV coating. The macrophage adhesion/activation and inflammatory cytokine release (tumor necrosis factor-alpha and interleukin-1) results indicated that the HA/ColV coating could significantly improve the anti-inflammation property of the Ti substrate. The *in vivo* implantation of SD rats for 3 weeks' results demonstrated that the HA/ColV coating caused milder tissue response. All these results suggested that the multi-functional HA/ColV coating possessed good biocompatibility. This research is anticipated to be potentially applied for the surface modification of cardiovascular stents.

Keywords: cardiovascular devices; biocompatibility; surface modification; hyaluronan; Type IV collagen

Introduction

Cardiovascular implant applied on the clinical treatment of cardiovascular disease (CVD) should perform its function with good blood compatibility, especially in the early stages after implantation [1]. The adsorption/conformational change of plasma proteins and the adhesion/activation of platelets on the device surfaces may induce thrombus formation and further implant failure [1]. Inhibition of inflammation is another consideration during the whole implantation process and posttreatment [2, 3]. The macrophages is one of the first cells to arrive at the tissue-implant-interface during the inflammation, and their attachment and activated by biomaterials can release chemotatic factors, adhesion molecules, chemokines and cytokines, such as tumor necrosis factor-alpha (TNF-α) and interleukin-1 (IL-1) [4]. During the implantation, macrophage aggregation and activation,

inflammatory cytokines release may induce pathological growth and migration of vascular smooth muscle cells (SMC) and endothelial cells (EC) at the diseased part and/or injured site of the vessel [5–7]. This process accompanied by disordered action of the clotting factor and the conformational change/agglomeration of fibrinogen may induce the events of in-stent thrombosis and intimal hyperplasia [8–10], and then long-term and more serious inflammation [11, 12], which is detrimental for the long-term interventional treatment of CVD [13, 14]. Tissue compatibility of the implanted devices should also be considered because the implantation may trigger undue host response, such as aggregation and proliferation of fibroblasts [15, 16], and further lead to the vascular wall thickening and luminal restenosis [17, 18]. Therefore, enhancing the blood compatibility, tissue compatibility and anti-inflammation of the implanted devices is overwhelmingly crucial for their clinical application.

Surface modification of biomaterials has been widely researched for the purpose of enhancing their biocompatibility [19–21]. Immobilizing endothelial extracellular matrix (ECM) components (collagen [22], fibronectin [23], laminin [24] and hyaluronan (HA)[25], etc.) and other biomolecules (heparin [26], gallic acid [27], dopamine [28] and chondroitin sulfate [29], etc.) on the biomaterials has been fully developed as a mature approach for surface modification of cardiovascular biomaterials. However, how to construct a multi-functional microenvironment which has outstanding biocompatibility using these biomolecules requires further investigation.

It has been reported the interaction with HA can make *in vitro* CoIV structure more ordered and biomimetic to the CoIV in the natrual vascular endothelial ECM [30]. In the previous work, we constructed a novel biocoating composed of hyaluronic acid (HA, 1×10^6 Da) and Type IV collagen (CoIV) [31, 32]. HA is a glycosaminoglycan which is one of main components of the EC ECM and owns multi-functional advantages for the application of biomedical materials, such as anti-coagulation [33], anti-inflammation [34] and anti-hyperplasia [35], etc. CoIV is another main ingredient of the EC ECM and constructs the skeleton of the EC ECM [36]. CoIV in natural ECM can improve EC attachment, proliferation and migration [37], meanwhile promote SMC contractile phenotype [31]. The previous constructed HA/CoIV coating has been proven better ability of anti-hyperplasia and endothelialization compared with the pure HA coating or CoIV coating, respectively [31, 32]. However, the effects of this multi-functional HA/CoIV coating on anti-coagulation and inhibition of inflammation have not been evaluated, and its *in vivo* tissue compatibility has also not been investigated.

In the present work, the blood compatibility (platelet adhesion/activation and the whole blood performance) and anti-inflammation property (macrophage adhesion/activation and inflammatory cytokines release) on the HA/CoIV coating were investigated, respectively (Fig. 1). In addition, subcutaneous implantation in SD rats was also investigated. We hope this HA/CoIV coating will not only be SMC and EC compatible but also blood and tissue compatible,
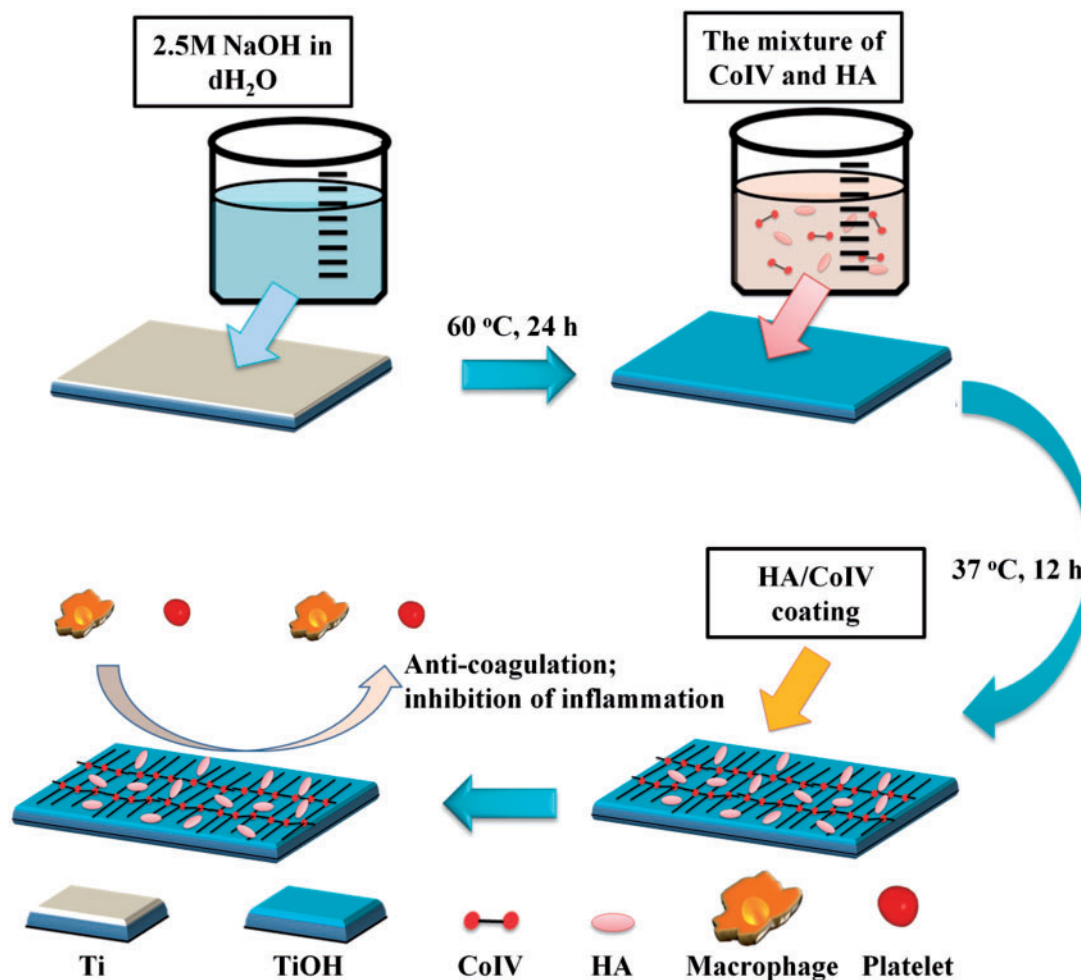

Figure 1. The scheme of preparing HA/PDA coating on Ti surface and its effect on anti-coagulation and anti-inflammation

which will be promising for the development of new generation of multi-functional and biocompatible cardiovascular devices.

Materials and experiments

Fabrication of the HA/CoIVcoating

The HA/CoIV coating was fabricated onto the 2.5 M NaOH treated titanium (Ti) substrate (labeled as TiOH) as our previous work described [31, 32]. Briefly, CoIV powder (Sigma, USA) was diluted to a concentration of 500 μg/ml with 5 mg/ml HA (Sangon Biological Engineering Co. Ltd, China) solution (deionized water) at pH 6.9. Then, the TiOH sample was immersed in this mixture and incubated for 12 h at 37°C. After the rinsed step (deionized water, three times, 5 min each time), the sample was dried at room temperature. TiOH samples immersed in 500 μg/ml CoIV solution (diluted in acetate buffer, pH 4) (labeled as CoIV/TiOH) and 5 mg/ml HA (labeled as HA/TiOH) incubated for 12 h at 37°C were used as control.

Fluorescence staining of CoIV on the HA/CoIVcoating

The fluorescence staining of CoIV on the HA/CoIV coating and CoIV/TiOH sample were performed using the related kits to observe the structure difference. This characterization was also used to confirm the successful preparation of the HA/CoIV coating on the TiOH surface.

Blood compatibility of the HA/CoIVcoating

The blood compatibility of the HA/CoIV coating was investigated by the platelet adhesion and the whole blood test, respectively, and the Ti, TiOH, CoIV/TiOH and HA/TiOH samples were used as control.

For the platelets adhesion test, fresh whole blood of a volunteer was centrifuged at 1500 rpm for 15 min to obtain the platelet-rich plasma (PRP), then the PRP was added to the samples surfaces and incubated at 37°C for 1 h. After washed with normal saline (NS, pH = 7.4) for three times (each time 5 min), the adherent platelets were fixed with 4% paraformaldehyde at 4°C for 2 h. The morphology of the adhered platelets was examined by a Rhodamine123 staining (Sigma, USA) and observed under a fluorescence microscope (DMRX, Leica, Germany) [38]. The amounts of the adherent platelets and the activated platelets were determined by the Lactate dehydrogenase (LDH) and GMP140 assay, respectively [39, 40].

For the whole blood test, the HA/CoIV and the control samples were set into a flow chamber device *in vitro*, and the whole blood flow with 15 dyn/cm^2 speed was applied in the devices at 37°C for 1 h. Then, the samples were taken out, washed with NS (pH = 7.4) for three times (each time 5 min) and fixed with 2.5% glutaraldehyde solution. After the rinsed and further dried step, the samples were coated with gold to conduct SEM to evaluate the morphology [41].

Anti-inflammation property of the HA/CoIVcoating

The amounts of the attached macrophages and their inflammatory cytokines were detected as the evaluation of the anti-inflammation property of the HA/CoIV coating in this study. The peritoneal macrophages extracted from the SD rats were obtained as the previous work described [33] and cultured at 37°C in a humidified atmosphere containing 95% air and 5% CO$_2$. Replicated cultures were performed when cells approached confluence, and cells were fed with fresh prepared growth medium every 48 h. The cells were added onto each samples with the concentration of 5×10^4 cells/ml and incubated at 37°C for 24 h. To study the extent of cell morphology and spreading, a Rhodanmine123 staining was used for the attached macrophages, and the numbers of the cells on each samples were statistically counted from at least 15 random pictures [42]. The supernatant harvested after macrophages cultured on samples for 24 h was applied as the specimen, and the TNF-α and IL-1 release were measured using related kits according to the manual [4]. All the inflammatory cytokines were finally normalized to the cell number.

In vivo tissue response test of HA/CoIVcoatings

In this study, three adult SD rats weighing ~0.4 kg were used. The double mirror-polished bare Ti disks (diameter = 10 mm, $n = 3$), TiOH disks (diameter = 10 mm, $n = 3$), HA coated TiOH disks (diameter = 10 mm, $n = 3$), CoIV coated TiOH disks (diameter = 10 mm, $n = 3$) and HA/CoIV coated disks (diameter = 10 mm, $n = 3$) were subcutaneously implanted on the back of both sides. After 3 weeks, the tissue around the implanted samples was harvested to evaluate the *in situ* body response reaction. The harvested tissue was fixed in 10% formaldehyde for 4–5 days. After washing by NS, the harvested tissue was then dehydrated in graded ethanol, saturated with xylene and embedded in paraffin. Hematoxylin and eosin (HE) staining of paraffin sections were performed for further histological analysis [15].

Statistical analysis

The data were statistically evaluated using analysis of variance (ANOVA) by homogeneity test of variances first, and *post hoc* test was prepared subsequently in Fisher's Least Significant Difference (statistics; analysis) (LSD) method for comparison. They were expressed as mean ± SD. The probability value $P < 0.05$ was considered as a significant difference. The data analysis was performed using the software SPSS 11.5 (Chicago, IL).

Results and discussion

Quality characterization of the HA/CoIVcoating

Figure 2 depicts the immunofluorescence images of CoIV on CoIV/TiOH and HA/CoIV samples. The CoIV exhibited distribution in dispersed clusters on CoIV/TiOH surface, whereas showed mesh-like distribution with microscopically visible fibers on the CoIV/HA coated surfaces, and the diameter of the mesh ranged from 20 to 30 μm which might contributed to the migration of EC. On the HA/CoIV coating, several oriented microstripes could also be seen clearly, and this structure was able to induce EC biomimetic elongation to release more anti-coagulant factor, such as nitric oxide, prostacyclin and thrombomodulin [32]. The results above not only indicated the successful preparation of the HA/CoIV coating on the TiOH surface but also proved that the mixture of CoIV and HA made the CoIV distribution more ordered and biomimetic.

Hemocompatibility of the HA/CoIVcoating

The *in vitro* platelet adhesion test was used to investigate the hemocompatibility of the HA/CoIV coating preliminarily. The representative fluorescence images of platelets adhesion behavior on these surfaces are depicted in Fig. 3A. Platelets attached and aggregated markedly on Ti substrate, TiOH sample and CoIV/TiOH sample with marked shape change (spreading) and pseudopod formation,
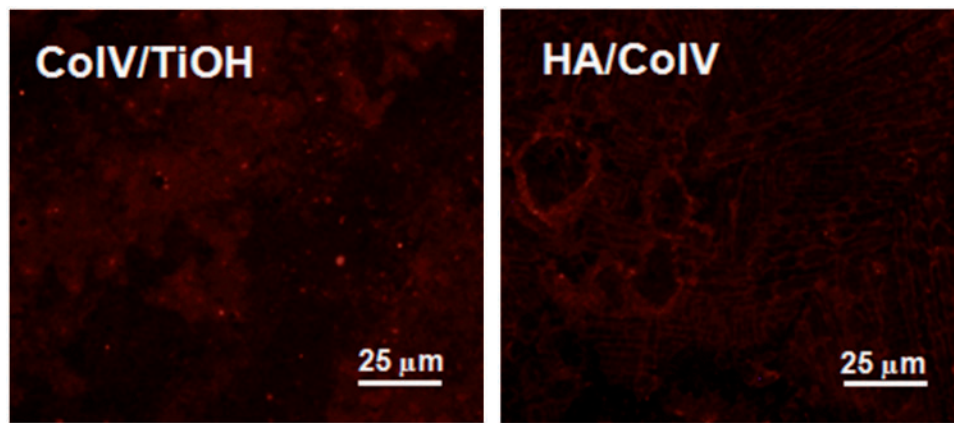
Figure 2. Immunofluorescence staining images of ColV on the samples of ColV/TiOH and HA/ColV
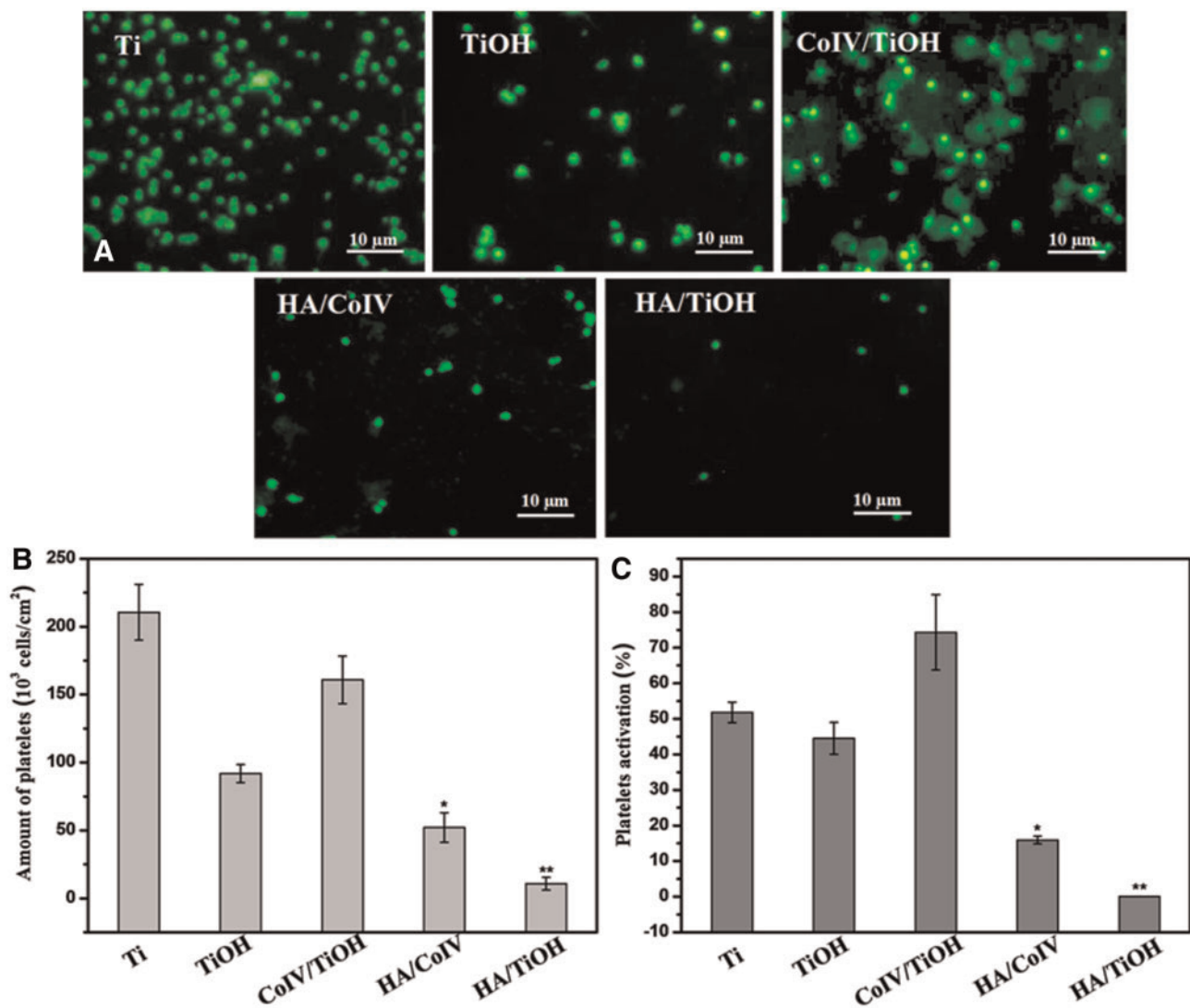

Figure 3. (**A**) Fluorescence images of platelets on the samples of Ti, TiOH, ColV/TiOH, HA/ColV and HA/TiOH; amounts of (**B**) attached and (**C**) activated platelets on the samples of Ti, TiOH, ColV/TiOH, HA/ColV and HA/TiOH (*$P < 0.05$ compared with Ti, TiOH and ColV/TiOH, **$P < 0.05$ compared with Ti, TiOH, ColV/TiOH and HA/TiOH, mean $\pm$ SD, $n = 3$)
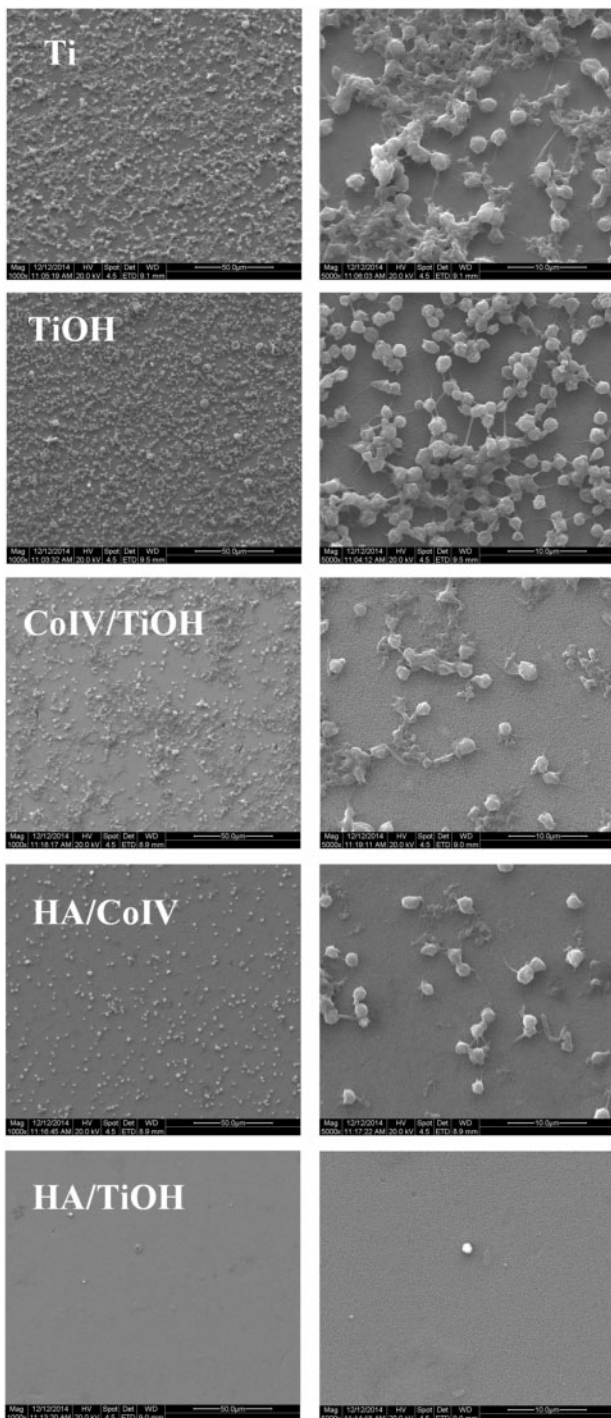
Figure 4. Typical SEM photograph of the whole blood ingredient attached on the samples of Ti, TiOH, CoIV/TiOH, HA/CoIV and HA/TiOH under a 15 dyn/cm² BFSS for 1 h

especially the platelets attached on the CoIV/TiOH, exhibited complete spreading morphologies, indicating serious activation. However, adhesion and aggregation of the platelets on HA/CoIV coating and HA/TiOH sample were significantly reduced for the presence of HA, and platelets on the HA conjugated sample maintained their round shapes with no formation of pseudopods. The quantity of platelets on different samples detected by the LDH method was presented in Fig. 3B. The data showed that the Ti

substrate, TiOH sample and CoIV/TiOH sample facilitated a much higher level of platelet adhesion compared with samples of HA/CoIV coatings and HA/TiOH ($P < 0.05$). The quantity of adhered platelets on all the samples increased in the order: HA/TiOH< HA/CoIV coating < TiOH < CoIV/TiOH < Ti. The activated ratio of the adherent platelet on different samples examined by the GMP140 assay was displayed in Fig. 3C. The quantity of activated platelets was in consistent with the fluorescence images, and increased in the order: HA/TiOH< HA/CoIV coating < Ti and TiOH < CoIV/TiOH. It was clear that the platelets on the CoIV/TiOH possessed the biggest activated ratio, while it was interesting that the more CoIV on the HA/CoIV coating (description in the previous work [31, 32]) didn't make more activation. More HA amount on the HA/CoIV coating provided the most contribution [31, 32] but the ordered CoIV distribution might be another important reason [33].

To investigate the overall hemocompatibility of the HA/CoIV coating in further, the whole blood test under a biomimetic blood flow (BFSS: 15 dyn/cm²) was performed, and the representative typical SEM images were depicted in Fig. 4. It was remarkable that there were lots of fibers, red blood cells (RBC) and activated platelets attached on the bare Ti, TiOH and CoIV/TiOH samples. The platelets gathered, outstretched their pseudopod and intertwined with a large number of fibers. However, the attachment of fibers, platelets and RBC on HA/CoIV and HA/TiOH samples were significantly reduced. All these results indicated that the HA/CoIV coating possessed better hemocompatibility compared with the bare Ti, TiOH and CoIV/TiOH samples but not enough compared with the HA/TiOH sample.

Anti-inflammation property of the HA/CoIVcoating

For the biomedical implanted devices, it is an important criterion of macrophage adhesion, activation and inflammatory cytokine release for judging the degree of inflammatory response [4]. Thus, the attachment, activation and inflammatory cytokine release (TNF-α and IL-1) of the macrophages were performed to investigate the anti-inflammation property of the HA/CoIV coating. Obviously, the macrophages on the HA/CoIV coating presented round and shrinked morphology, suggesting non-activated phenotype, while the macrophages on the Ti, TiOH, CoIV/TiOH and HA/TiOH samples polygonal and spreading morphology, and this indicated the activated phenotype (Fig. 5A). The attached and activated macrophages on the HA/TiOH surface may be attributed to the exposure of the TiOH substate, which indicated the inhomogeneous distribution of the HA on the HA/TiOH surface. From the statistical count results of macrophages on each sample in Fig. 5B, the HA/CoIV coating and HA/TiOH sample exhibited significantly less adherent macrophages compared with Ti, TiOH and CoIV/TiOH samples. These results indicated that the HA/CoIV coating could inhibit macrophage adhesion and activation effectively. Figure 6 presents the expression of TNF-α and IL-1 released by macrophages after 24 h incubation on various samples. It was clear that the CoIV/TiOH surface showed more expression of TNF-α and IL-1, which indicated more activation of the macrophages, while the HA/TiOH surface showed almost no expression of the inflammatory cytokines, and the reason might be that there were too few macrophages attached on the HA/TiOH surface, thus the cytokines could not be detected. It had been reported that HA could effectively suppress adhesion, activation and inflammatory cytokines of the macrophages, thus possessed excellent anti-inflammation function [43]. It was notable that the HA/CoIV coating presented significantly less expression of TNF-α and IL-1 compared with CoIV/TiOH, Ti and TiOH samples attributing to the more HA immoblized on the coating. All the result indicated that the HA/CoIV coating could effectively enhance the anti-inflammation property of the surface.
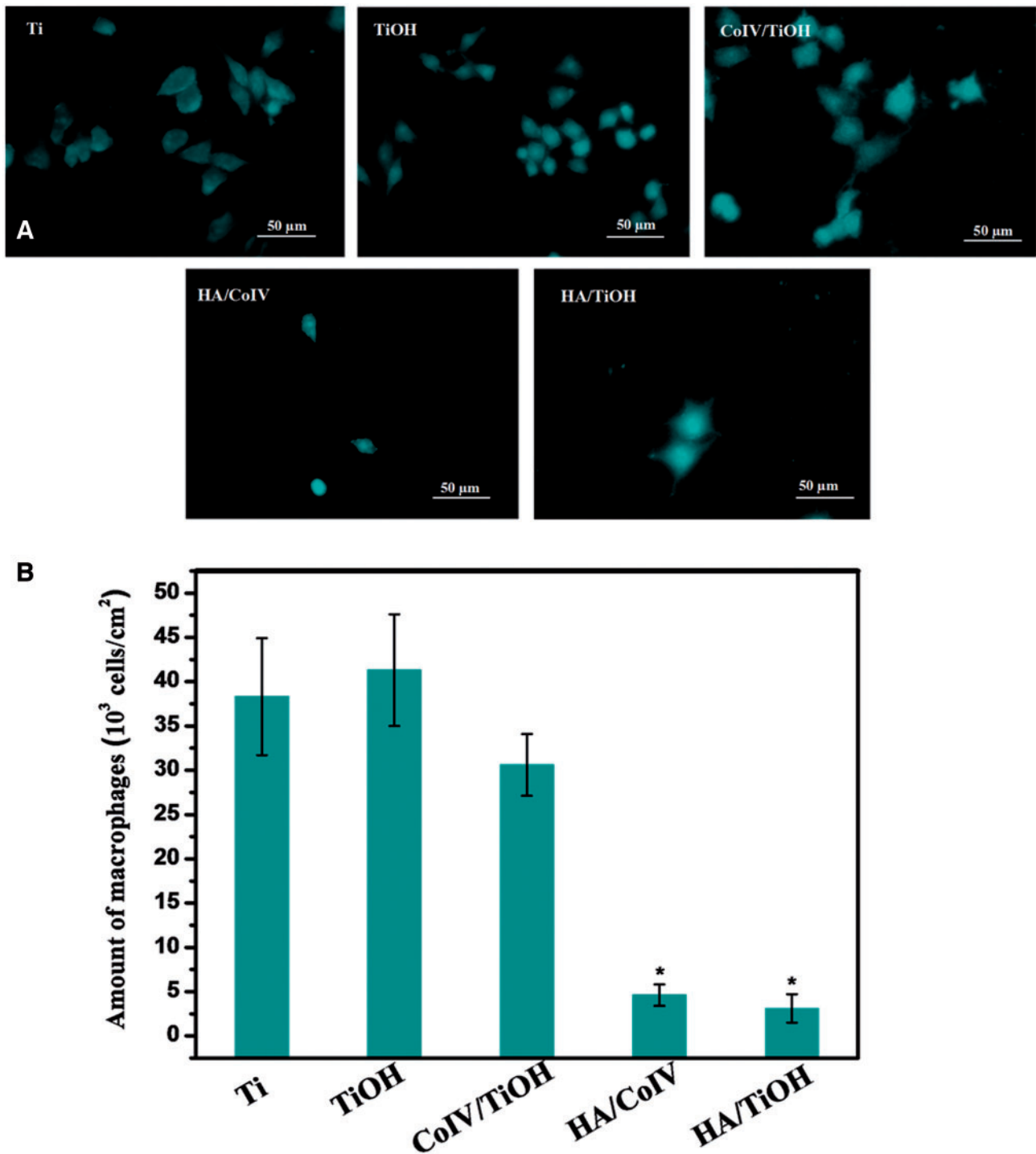
Figure 5. (**A**) Fluorescence images and (**B**) counts of attached macrophages on the samples of Ti, TiOH, CoIV/TiOH, HA/CoIV and HA/TiOH after incubation for 24 h (*$P < 0.05$ compared with other samples, mean ± SD, $n = 3$)

In vivo tissue response test of HA/CoIV coating

When a biomedical device is implanted inside the patient, good tissue compatibility is required, because the local tissue response may influences its safety and performance *in vivo* [44, 45]. To fully rate the tissue response to HA/CoIV coating, samples were implanted subcutaneously implantation in SD rats. After 3 weeks, the tissue around the implant site was harvested for *in situ* analysis. HE (Fig.

7) of sections were performed for histological analysis. Neither bare Ti nor the HA/CoIV samples induced local toxic reactions. There were less inflammatory cell infiltration and granulation tissue development presented on HA/CoIV sample and HA/TiOH sample. The introduction of the HA/CoIV altered the tissue response but did not completely suppress fibrous capsule formation. For the Ti and TiOH substrates, the thickness of fibrous encapsulation surrounding
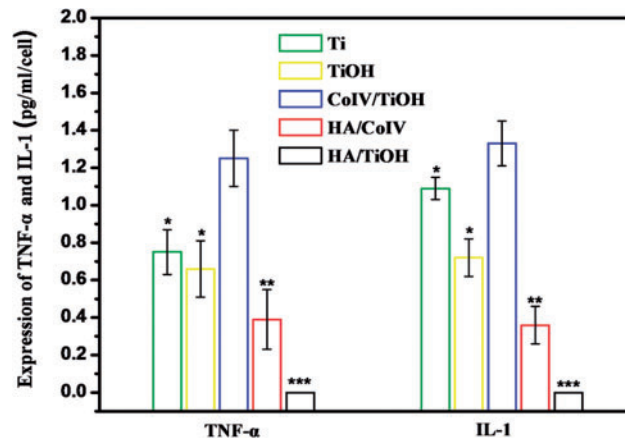
Figure 6. The amounts of (**A**) TNF-α and (**B**) IL-1 released from attached macrophageson the samples of Ti, TiOH, CoIV/TiOH, HA/CoIV and HA/TiOH after incubation for 24 h (*$P < 0.05$ compared with CoIV/TiOH, **$P < 0.05$ compared with Ti, TiOH and CoIV/TiOH, ***$P < 0.05$ compared with the other samples, mean ± SD, $n = 3$)
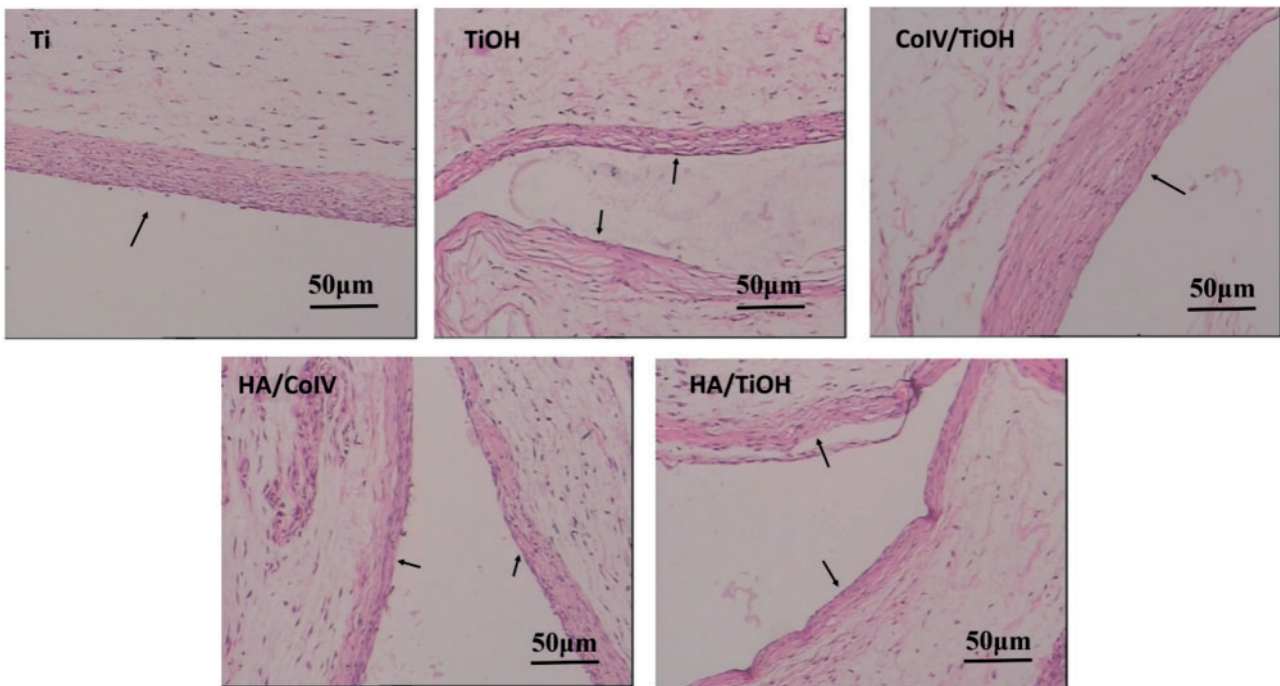

Figure 7. HE staining for subcutaneous tissues around Ti, TiOH, CoIV/TiOH, HA/CoIV and HA/TiOH after 3 weeks, respectively

the implanted site was 46.6 ± 3.6 μm and 21.5 ± 5.5 μm, respectively, at 3 weeks, while the thickness reduced to 20.8 ± 4.7 μm after coated with HA/CoIV, or 25.4 ± 4.4 μm after immobilized with HA. Although for the CoIV coated TiOH, the thickness significantly increased to 76.7 ± 1.6 μm, suggesting a more serious tissue response. It was included that the HA/CoIV coating showed acceptable and attenuated tissue response compared with the other samples, with less inflammatory cell infiltration, granulation tissue formation and thinner fibrous capsule development.

Conclusion

In the present work, the micromesh structure composed of HA and CoIV (HA/CoIV coating) was successfully prepared onto the TiOH surface. Platelet adhesion/activation and the dynamic whole blood test indicated that the HA/CoIV coating possessed better blood compatibility compared with Ti, TiOH and CoIV/TiOH surfaces. Macrophage adhesion/activation and TNF-α/IL-1 release results proved that the HA/CoIV coating could effectively suppress inflammation. Additionally, *in vivo* experiment demonstrated that the HA/CoIV coating made milder tissue response suggesting excellent tissue compatibility. Nevertheless, the drug loading and delivery ability of this HA/CoIV layer should still be investigated. Thus, in the future work, we will choose one or more functional drug (such as heparin or metal nano-particle) to load in the HA/CoIV coating to endow the coating better biocompatibility.

Acknowledgements

References

1. LiG C, Yang P, Liao YZ *et al*. Tailoring of the titanium surface by immobilization of heparin/fibronectin complexes for improving blood compatibility and endothelialization: an in vitro study. *Biomacromolecules* 2011; **12**:1155–68.

2. Patrick WS, Sigmund S, Scot G *et al*. Comparison of zotarolimus-eluting and everolimus-eluting coronary stents. *N Engl J Med* 2010; **363**:136–46.

3. Robert AM, Crawford AH, Ashley MM *et al*. Reducing in-stent restenosis: therapeutic manipulation of miRNA in vascular remodeling and inflammation. *J Am Coll Cardiol* 2015; **65**: 2314–27.

4. Li GC, Yang P, Guo X *et al*. An in vitro evaluation of inflammation response of titanium functionalized with heparin/fibronectin complex. *Cytokine* 2011; **56**:208–17.

5. Stankevich KS, Gudima A, Filimonov VD *et al*. Surface modification of biomaterials based on high-molecular polylactic acid and their effect on inflammatory reactions of primary human monocyte-derived macrophages: perspective for personalized therapy. *Mater Sci Eng C Mater Biol Appl* 2015; **51**:117–26.

6. Moore KJ, Tabas I. Macrophages in the pathogenesis of atherosclerosis. *Cell* 2011; **145**:341–55.

7. Chang HB, Tieyan H, Judy W *et al*. Txnip ablation reduces vascular smooth muscle cell inflammation and ameliorates atherosclerosis in apolipoprotein E knockout mice. *Atherosclerosis* 2015; **241**: 313–21.

8. Teruo I, Kevin C, Toshifumi M *et al*. Vascular inflammation and repair: implications for re-endothelialization, restenosis, and stent thrombosis. *JACC Cardiovasc Interv* 2011; **4**: 1057–66.

9. Marcin S, Michał Z, Anetta U. Coronary thrombus composition: links with inflammation, platelet and endothelial markers. *Atherosclerosis* 2014; **237**: 555–61.

10. Bimmer EC, José PSH, Farouc AJ *et al*. Stent thrombosis: a clinical perspective. *JACC Cardiovasc Interv* 2014; **7**: 1081–92.

11. Mohammed TA, Kenneth M, Arun HSK *et al*. A novel CX3CR1 antagonist eluting stent reduces stenosis by targeting inflammation. *Biomaterials* 2015; **69**:22–9.

12. Hung MJ, Hsu KH, Chang NC *et al*. Prevalence of coronary artery spasm after stent placement and its association with inflammation. *Int J Cardiol* 2015; **179**:252–5.

13. Manabu O, Katsumi M, Takatoshi K *et al*. Impact of preprocedural high-sensitive C-reactive protein levels on long-term clinical outcomes of patients with stable coronary artery disease and chronic kidney disease who were treated with drug-eluting stents. *J Cardiol* 2015; **66**: 15–21.

14. Kim S, Lee JH, Shin DH *et al*. Long-term outcomes of neointimal hyperplasia without neoatherosclerosis after drug-eluting stent implantation. JACC. *Cardiovasc Imaging* 2014; **7**: 788–95.

15. Yang Y, Qi PK, Ding YH *et al*. A biocompatible and functional adhesive amine-rich coating based on dopamine polymerization. *J Mater Chem B* 2015; **3**:72–81.

16. Yang Y, Qi PK, Wen F *et al*. Mussel-inspired one-step adherent coating rich in amine groups for covalent immobilization of heparin: hemocompatibility, growth behaviors of vascular cells, and tissue response. *Appl Mater Interfaces* 2014; **6**:14608–20.

17. Goel SA, Guo WL, Shi XD *et al*. Preferential secretion of collagen type 3 versus type 1 from adventitial fibroblasts stimulated by TGF-β/Smad3-treated medial smooth muscle cells. *Cell Signal* 2013; **25**: 955–60.

18. Kim IH, Ishihara K, Lee S *et al*. Tissue response to poly(l-lactic acid)-based blend with phospholipid polymer for biodegradable cardiovascular stents. *Biomaterials* 2011; **32**: 2241–7.

19. Lin P, Lin CW, Mansour R *et al*. Improving biocompatibility by surface modification techniques on implantable bioelectronics. *Biosens Bioelectron* 2013; **47**:451–60.

20. Lim IJ, Kim HJ. Enhanced biocompatibility and adhesive properties of modified allyl 2-cyanoacrylate-based elastic bio-glues. *Colloids Surf B Biointerfaces* 2015; **133**:19–23.

21. Xu ZK, Nie FQ, Qu C *et al*. Tethering poly(ethylene glycol)s to improve the surface biocompatibility of poly(acrylonitrile-co-maleic acid) asymmetric membranes. *Biomaterials* 2005; **26**: 589–98.

22. Cheng ZY, Teoh SH. Surface modification of ultra thin poly (ε-caprolactone) films using acrylic acid and collagen. *Biomaterials* 2004; **25**: 1991–2001.

23. Li GC, Yang P, Qin W *et al*. The effect of coimmobilizing heparin and fibronectin on titanium on hemocompatibility and endothelialization. *Biomaterials* 2011; **32**:4691–703.

24. Santiago LY, Nowak RW, Rubin JP *et al*. Peptide-surface modification of poly(caprolactone) with laminin-derived sequences for adipose-derived stem cell applications. *Biomaterials* 2006; **27**: 2962–9.

25. Ekaputra AK, Prestwich GD, Cool SM *et al*. The three-dimensional vascularization of growth factor-releasing hybrid scaffold of poly (ε-caprolactone)/collagen fibers and hyaluronic acid hydrogel. *Biomaterials* 2011; **32**: 8108–17.

26. Yang ZL, Tu QF, Wang J *et al*. The role of heparin binding surfaces in the direction of endothelial and smooth muscle cell fate and re-endothelialization. *Biomaterials* 2012; **33**: 6615–25.

27. Campoccia D, Montanaro L, Arciola CR. A review of the biomaterials technologies for infection-resistant surfaces. *Biomaterials* 2013; **34**: 8533–54.

28. Luo RF, Tang LL, Zhong S *et al*. In vitro investigation of enhanced hemocompatibility and endothelial cell proliferation associated with quinone-rich polydopamine coating. *ACS Appl Mater Interfaces* 2013; **5**:1704–14.

29. Liu YX, He T, Gao CY. Surface modification of poly(ethylene terephthalate) via hydrolysis and layer-by-layer assembly of chitosan and chondroitin sulfate to construct cytocompatible layer for human endothelial cells. *Colloids Surf B: Biointerfaces* 2005; **46**: 117–26.

30. Schanté CE, Zuber G, Herlin C *et al*. Chemical modifications of hyaluronic acid for the synthesis of derivatives for a broad range of biomedical applications. *Carbohydr Polym* 2011; **85**: 469–89.

31. Li JA, Zhang K, Chen HQ *et al*. A novel coating of type IV collagen and hyaluronic acid on stent material-titanium for promoting smooth muscle cell contractile phenotype. *Mater Sci Eng C* 2014; **38**:235–43.

32. Li JA, Zhang K, Wu F *et al*. Constructing bio-functional layers of hyaluronan and type IV collagen on titanium surface for improving endothelialization. *J Mater Sci* 2015; **50**:3226–36.

33. Li JA, Zhang K, Wu JJ *et al*. Tailoring of the titanium surface by preparing cardiovascular endothelial extracellular matrix layer on the hyaluronic acid micro-pattern for improving biocompatibility. *Colloids Surf B Biointerfaces* 2015; **128**:201–10.

34. Zhang HQ, Huang SL, Yang XY *et al*. Current research on hyaluronic acid-drug bioconjugates. *Eur J Med Chem* 2014; **86**:310–7.

35. Freudenberger T, Dai G, Mayer P *et al*. P359 lentiviral overexpression of hyaluronic acid synthases 1 and 2 restores estradiol-mediated inhibition of PDGF-induced proliferation in vascular smooth muscle cells. *Atheroscler Suppl* 2010; **11**: 93

36. Murasawa Y, Hayashi T, Wang PC. The role of type V collagen fibril as an ECM that induces the motility of glomerular endothelial cells. *Exp Cell Res* 2008; **314**: 3638–53.

37. Heo Y, Shin YM, Lee YB *et al*. Effect of immobilized collagen type IV on biological properties of endothelial cells for the enhanced endothelialization of synthetic vascular graft materials. *Colloids Surf B Biointerfaces* 2015; **134**:196–203.

38. Xiang LJ, Li CH, Yang P *et al*. Fabrication of micro-patterned titanium dioxide nanotubes thin film and its biocompatibility. *J Eng* 2014; **7** doi:10.1049/joe.2014.0274.

39. Li JA, Zhang K, Yang P *et al*. Human vascular endothelial cell morphology and functional cytokine secretion influenced by different size of HA micro-pattern on titanium substrate. *Colloids Surf B Biointerfaces* 2013; **110**:199–207.

40. Li JA, Zhang K, Xu Y *et al*. A novel coculture model of HUVECs and HUASMCs by hyaluronic acid micropattern on titanium surface. *J Biomed Mater Res A* 2014; **102**:1950–60.

41. Xiang LJ, Li JA, He ZK *et al*. Design and construction of TiO$_2$ nanotubes in microarray using two-step anodic oxidation for application of cardiovascular implanted devices. *Nano Lett* 2015; **10**: 287–91.

42. Li JA, Yang P, Zhang K *et al*. Preparation of SiO$_2$/TiO$_2$ and TiO$_2$/TiO$_2$ micropattern and their effects on platelet adhesion and endothelial cell regulation. *Nucl Instrum Methods Phys Res B* 2013; **307**:575–9.

43. Gocmen G, Gonul O, Oktay NS *et al*. The antioxidant and anti-inflammatory efficiency of hyaluronic acid after third molar extraction. *J Cranio-Maxillofac Surg* 2015; **43**: 1033–7.

44. Fulco I, Miot S, Haug MD *et al*. Engineered autologous cartilage tissue for nasal reconstruction after tumour resection: an observational first-in-human trial. *Lancet* 2014; **384**: 337–46.

45. Wan Y, Mahmood MAI, Li N *et al*. Nanotextured substrates with immobilized aptamers for cancer cell isolation and cytology. *Cancer* 2012; **118**: 1145–54.